

Improving the diagnostic reliability of AE-based failure mode detection and distinction in CFRP

Jonathan Liebeton, Stella Mei Sze Soon, Dirk Söffker

Chair of Dynamics and Control, University of Duisburg-Essen, Germany.

E-mail: jonathan.liebeton@uni-due.de, stella.soon@stud.uni-due.de, soeffker@uni-due.de

The usage of carbon fiber reinforced plastics (CFRP) in safety critical systems requires the application of Structural Health Monitoring (SHM). A well-known non-destructive testing (NDT) method is Acoustic Emission (AE). AE-based methods enable a continuous and in-situ monitoring of CFRP structures. While the classification of damages using AE signal features is thoroughly studied, the investigation of the correlation between the reliability of classification results and the applied loading patterns enables a new metric to ensure the success of SHM methods. In this contribution the probability of detection is used to evaluate the reliability of classification results. The four damage modes (debonding, delamination, matrix crack, and fiber breakage) are classified by a support vector machine (SVM). To distinguish the damage modes time-frequency domain features of the corresponding AE signal are calculated and finally classified to evaluate the dependency between the applied loading patterns and the classification quality. A concept of an online control loop is proposed using the reliability of classification results as control variable for improved testing strategies finally leading to ensure a safe usage of CFRP structures.

Keywords: Reliability, Diagnostics, Structural Health Monitoring, Acoustic Emission, Online Testing.

1. Introduction

The increasing complexity of industrial plants requires SHM to ensure a safe operating system. The use of NDT methods is essential for monitoring systems and by applying the AE method, in-situ monitoring is possible. The method discussed in this paper is based on the analysis of a system's state of health by means of ultrasonic waves. If a damage occurs, energy is released as ultrasonic waves that propagate within the material and can be measured by piezoelectric transducers. Because the ultrasonic waves are generated by the material itself, AE is considered as a passive monitoring method.

The usage of monitoring systems in complex or remote plants can improve the efficiency. When CFRP is used as a lightweight substitute of equivalent strength for metals, SHM is required because of the material's non-ductile behavior. In case of offshore wind farms maintenance costs are the main factor behind high power generation costs (Tusar and Sarker (2022)). The remote location and weather dependent accessibility of offshore wind turbines lead to longer downtime. To decrease downtime and maintenance costs new

maintenance strategies are developed that rely on monitoring systems to define maintenance schedules when or before failures occur (Ren et al. (2021)). The overall efficiency can only be improved, if the information of the monitoring systems about the plant are reliable (Colone et al. (2019)).

The reliability of diagnostic statements, especially in the case of fault diagnosis, is analyzed in Rothe et al. (2017). It is shown, that the classification performance depends on systems loading conditions and the reliability of classification results can be improved by fusion of results of several classifiers.

The classification of damage mechanisms in CFRP is thoroughly studied. Features of time-frequency and frequency domain are commonly used for distinguishing between the damage mechanisms (Baccar and Söffker (2017)). The damage mechanisms are assigned to specific frequency ranges, which lie between 10 and 500 kHz. Delamination describes the detachment of single fiber layers and is observed at the lowest frequency range compared to the other damage mechanisms. In Hamdi et al. (2013) delamina-

tions are detected at frequencies of 30 to 90 kHz while in Gutkin et al. (2011) frequencies of 50 to 150 kHz are reported. Frequencies above the frequency range of delamination are associated with matrix cracks. In Oskouei et al. (2012) and Azadi et al. (2019) matrix cracks are denoted to frequencies in the range of 100 to 250 kHz. The loss of adhesion between matrix and fiber is characterized as debonding and is observed at the frequency range between matrix crack and fiber breakage. In Marec et al. (2008) debonding is observed at 170 to 350 kHz and in Nazmdar Shahri et al. (2016) at 250 to 310 kHz. Fiber breakage is unanimously reported at the highest frequency range. In Chelliah et al. (2019) a frequency range of 280 to 400 kHz is stated, while a frequency range of 420 to 500 kHz is observed by Sayar et al. (2018). The frequency ranges differ depending on the material properties, but the relative frequency order is not changing.

In Wirtz et al. (2016), the dependence between the loading conditions and the classification results is studied for the first time, and in Wirtz et al. (2019) it is further elaborated. While CFRP specimen are under cyclic load, AE are measured. The probability estimations are analyzed with respect to excitation frequencies and displacements. A direct relationship between loading condition and classification results can not be formulated.

This contribution is structured as follows: in section 2 the experimental set-up and procedure is introduced, followed by the applied methods to analyze the measurement data. The results of data analysis and machine learning are explained in section 4. In section 5 and section 6, summary and outlook are given.

2. Experiments

The experiments are divided into two phases, namely the initial damage phase and the cyclic loading phase. In the initial damage phase the CFRP specimen are damaged by indentation and during the cyclic loading phase the specimen are bent at various frequency and amplitude combinations. The experimental procedure is first described in Wirtz et al. (2019). In comparison to Wirtz et al. (2019) the set-up is changed for spec-

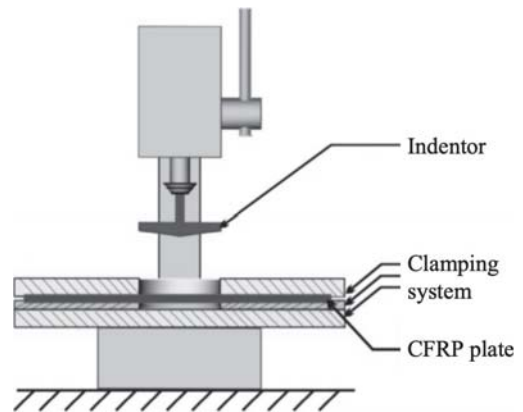


Fig. 1. Experimental set-up for indentation Baccar and Söffker (2017)

imen of shorter length and the displacement is not used as control parameter, because the material stiffness is decreasing with material degradation (Wang and Zhang (2020)). Therefore, a constant displacement would lead over time to a decreasing load. Instead of the displacement the input amplitude of the power supply is controlled to ensure a constant loading conditions. The CFRP plates have the dimensions $130 \times 60 \times 2$ mm and consist of three layers in $90^\circ/0^\circ/90^\circ$ orientation. In both experiment phases, the occurring AE are measured by piezoelectric transducers, using the piezoelectric effect to convert surface displacements into voltage signals. A preamplifier with high input impedance and low output impedance ensures that the transducers are not affected by the sampling of the signal. The analog voltage signal is digitized using a field programmable gate array measurement board with a sampling frequency of 4 MHz and 16-bit resolution (Dettmann (2012)).

First initial damages are induced by indentation. The experimental set-up is shown in figure 1 and is described by Baccar and Söffker (2017). The CFRP specimen are secured by a clamping system and a conical indenter with obtuse angle and a diameter of 100 mm is used to apply bending loads. A second indenter with smaller diameter and acute angle is used to simulate impact damages and directly damage the matrix.

In the second phase of the experiment, the pre-

damaged specimens are clamped by a fixture on the slider and a stationary bench vise. The test rig is shown in figure 2 and used to apply different bending loads on the specimen. The power supply is controlled by a voltage sine signal and converts the voltage signal into a proportional current signal with constant voltage. The chosen frequencies and amplitudes of the sine signal are 2 to 6 Hz and 2 to 6 V, respectively. The actuator drives a crank which is connected to a slider. Thus the rotatory motion is converted into a translatory motion. The slider's displacement is measured by a proximity sensor. The measured displacements range from 6 to 10 mm. By controlling the input voltage instead of the resulting displacement a constant excitation force is ensured.

3. Methods

The raw AE data are preprocessed to filter out relevant AE events. The detection of signal parts containing damage related AE is done by analyzing signal energy in the frequency range of 10 to 500 kHz. Therefore, the short-time Fourier transform (STFT) of the measurement data is calculated. The STFT of a signal $x(t)$ is defined as

$$X_F(\omega, \tau) = \int_{-\infty}^{\infty} x(t)\gamma(t-\tau)e^{-j\omega t} dt, \quad (1)$$

where $\gamma(t-\tau)$ denotes the window function of the local Fourier spectrum at time τ .

The calculated coefficients at the given frequency range are used to calculate the signal energy for each time window at the given frequency range. Threshold monitoring is applied to detect high energy signal parts. The corresponding signal part in time domain is manually analyzed and labeled. Labeling is based on the criteria of the respective damage mechanisms described in section 1. For feature extraction the continuous wavelet transform (CWT) is calculated for each detected and labeled AE signal. The CWT of a signal $x(t)$ is defined as

$$X_W(s, \tau) = \frac{1}{\sqrt{s}} \int_{-\infty}^{\infty} x(t)\Psi^*\left(\frac{t-\tau}{s}\right) dt \quad (2)$$

with the wavelet Ψ^* , frequency-scale parameter s and time-scale parameter τ .

The CWT coefficients of the time window with the highest CWT coefficient is used as feature vector. Here, only the CWT coefficients corresponding to the frequency range of 10 to 500 kHz are considered. This leads to a feature vector of 60 elements.

A SVM is a binary classifier separating two classes of data by a linear hyperplane. The internal optimization problem is the maximization of the margin, the distance between the support vectors (SVs) of each class. In case of not linear separable data, the feature space is transformed by kernel functions. To use a SVM for multi-class classification two strategies can be applied.

The One-Against-All (OAA) strategy separates each class from every other class of the classification problem. The number of required SVMs N_{OAA} is equal to the number classes C . The One-Against-One (OAO) strategy separates two individual classes from each other. Therefore the number of required SVMs N_{OAO} is higher for more than three classes in comparison to the OAA and defined by

$$N_{OAO} = \frac{C(C-1)}{2}. \quad (3)$$

For both strategies the class of an unknown data sample is predicted by determining the highest decision value among all SVMs (Sharmila Joseph et al. (2022)).

The decision value f is used to calculate the posterior probability r_{ij} of class i and binary classifier j by

$$r_{ij} = \frac{1}{1 + e^{Af+B}}, \quad (4)$$

where the estimations of A and B are calculated by minimizing the negative log likelihood of training data (Chang and Lin (2011))(Platt (1999)). The estimated probability p_i is calculated by solving the quadratic approach of Wu et al. (2004)

$$\min_p \frac{1}{2} \sum_{i=1}^N \sum_{j:j \neq i} (r_{ji}p_i - r_{ij}p_j)^2, \quad (5)$$

where $p_i \geq 0, \forall i$, and $\sum_{i=1}^N p_i = 1$.



Fig. 2. Experimental set-up for cyclic loading

The probability p_i describes the affiliation of a data sample to class i .

4. Results

The SVM's hyperparameter are optimized using Bayesian optimization. A training data set of 100 data samples per class is used to train the classification algorithm. Over-fitting during the training process is avoided by 10-fold cross-validation. The best validation results are achieved with a linear kernel and the OAA strategy. The model's cross-validation accuracy is 95 %.

In the measurements during cyclic loading of the CFRP specimen 211 damages are detected. For several frequency-displacement and frequency-voltage combinations no damage mechanisms are detected. With 45 % of all damage mechanisms delamination is the most frequently detected, followed by fiber breakage, matrix crack, and debonding with 22, 21, and 12 %, respectively.

The probability estimation for each damage is calculated. When several damage mechanisms of the same class are detected at the same frequency-displacement and frequency-voltage combination, the average probability estimation is calculated. The calculated probability estimations are visualized in figure 3 and 4 and denoted by the color code. For frequency-displacement and frequency-

voltage combinations, where no damage is detectable, the probability estimation is 0 %. In figure 4 probability estimations of each damage class are shown with respect to excitation frequency and displacement.

Beside of the frequency-displacement combinations 2 Hz and 10 mm, 5 Hz and 6 mm, and 6 Hz and 9 to 10 mm the probability estimations of delamination are calculated for the entire frequency-displacement field. The largest area of high probabilities are found at 2 to 4 Hz and 6 to 8 mm. Decreasing probabilities are observed at the combination of low frequencies and high displacements.

The largest area of high probabilities for matrix crack is at 4 to 5 Hz and 9 to 10 mm. Local probability maxima are observable at frequency-displacement combinations 6 Hz and 6 mm, 2 Hz and 7 and 9 mm, and 3 Hz and 8 mm. The remaining field shows lower probabilities.

The highest probabilities of debonding are at the frequency-displacement combinations 2 Hz and 8 to 9 mm, 4 Hz and 6 to 7 mm, and 6 Hz and 8 mm. Also in Wirtz et al. (2019) not all frequency-displacement combinations show detected damages.

For fiber breakage two larger areas of high probabilities are observed at frequency-

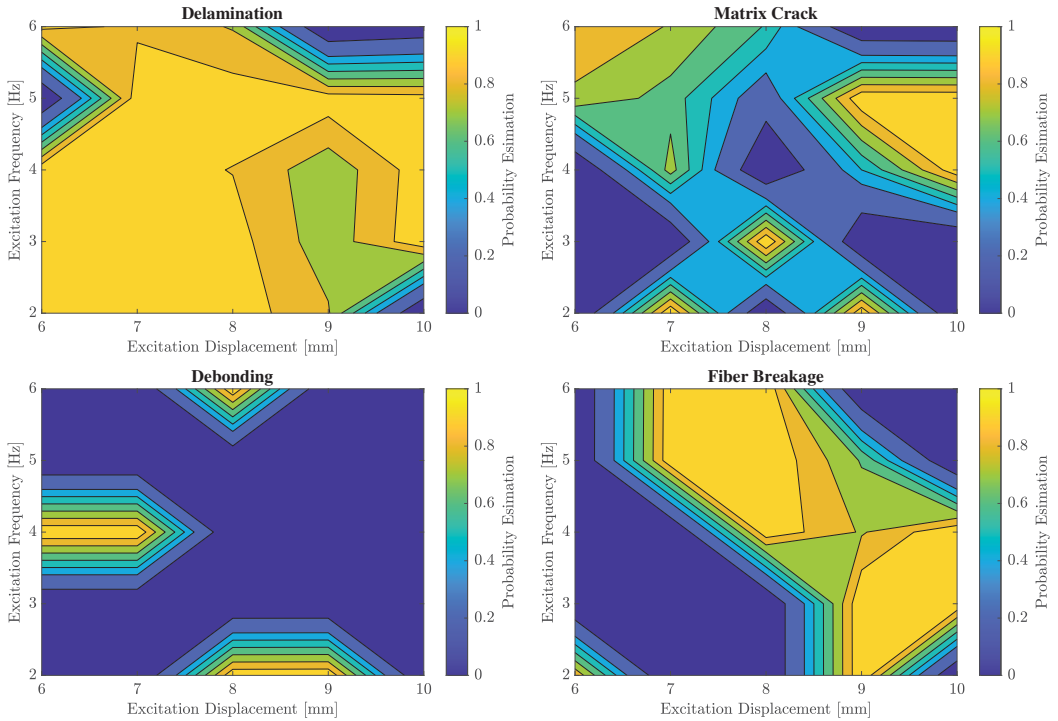


Fig. 3. Probability estimations depending on frequency and displacement

displacement combinations 4 to 6 Hz and 7 to 8 mm, and 2 to 4 Hz and 9 to 10 mm. The frequency-displacement combinations between the two fields show a decreasing probability.

The probability estimations with respect to excitation frequency and excitation voltage are shown in figure 4.

The highest probability for delamination is observable at frequency-voltage combinations of 2 to 5 Hz and 2 to 4 V.

At the frequency-voltage combination 3 to 6 Hz and 2 to 4 V a larger area of lower probabilities for matrix crack is displayed. A local maxima is located at 3 Hz and 5 V.

For fiber breakage a large area of high probability is shown. The highest probabilities can be found at high frequencies and low amplitudes, and at low frequencies and high amplitudes.

Similar probability distributions between frequency-voltage and frequency-displacement are observable, especially for debonding and fiber

breakage. The probability estimations with respect to the excitation frequency and the excitation voltage are more uniformly distributed than the probability estimations with respect to excitation frequency and displacement.

5. Summary

The results confirm a dependency between the reliability of classification results and loading conditions under which the damages arise and therefore will become theoretically detectable. Therefore, the reliable use of monitoring systems is limited as detection rates vary with loading conditions. If possible, systems can be operated under loading conditions, at which reliable diagnostic statements are generated, to increase the overall efficiency. In this way, downtime due to maintenance scheduled because of false detection of faults can be minimized while saving resources.

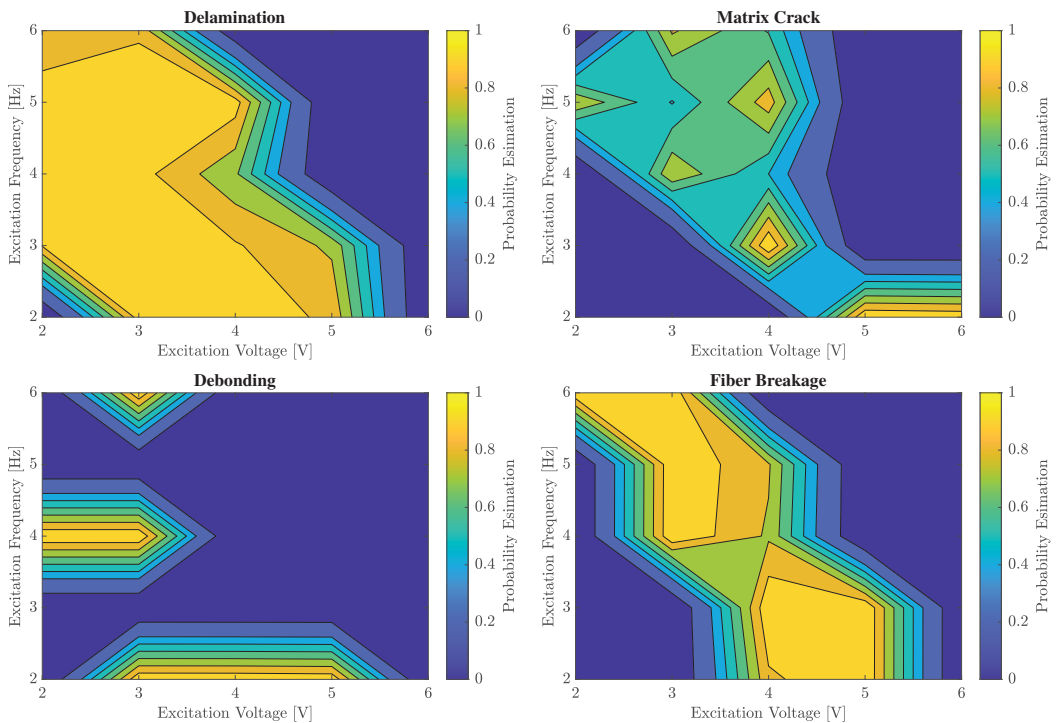


Fig. 4. Probability estimations depending on frequency and input voltage

6. Outlook

In future work the dependency between the reliability of the classification results and loading conditions has to be studied in more detail to establish a relationship between the excitation amplitude and frequency and the detection and classification of damage mechanisms. Finally, the measured AE signals can be classified online to establish a closed control loop. The control loop can be used to automatically adjust the loading conditions to an excitation amplitude and frequency combination under which the most reliable classification results can be obtained.

References

- Azadi, M., H. Sayar, A. Ghasemi-Ghalebahman, and S. M. Jafari (2019). Tensile loading rate effect on mechanical properties and failure mechanisms in open-hole carbon fiber reinforced polymer composites by acoustic emission approach. *Composites Part B: Engineering* 158, 448–458.
- Baccar, D. and D. Söffker (2017). Identification and classification of failure modes in laminated composites by using a multivariate statistical analysis of wavelet coefficients. *Mechanical Systems and Signal Processing* 96, 77–87.
- Chang, C.-C. and C.-J. Lin (2011). Libsvm: A library for support vector machines. *ACM Transactions on Intelligent Systems and Technology* 2(3), 1–27.
- Chelliah, S. K., P. Parameswaran, S. Ramasamy, A. Vellayaraj, and S. Subramanian (2019). Optimization of acoustic emission parameters to discriminate failure modes in glass–epoxy composite laminates using pattern recognition. *Structural Health Monitoring* 18(4), 1253–1267.
- Colone, L., N. Dimitrov, and D. Straub (2019). Predictive repair scheduling of wind turbine drive–train components based on machine learning. *Wind Energy* 22(9), 1230–1242.
- Dettmann, K.-U. (2012). Probabilistic-based method for realizing safe and reliable mecha-

- tronic systems. Dr.-Ing. dissertation, University of Duisburg-Essen.
- Gutkin, R., C. Green, S. Vangrattanachai, S. Pinho, P. Robinson, and P. Curtis (2011). On acoustic emission for failure investigation in CFRP: Pattern recognition and peak frequency analyses. *Mechanical Systems and Signal Processing* 25(4), 1393–1407.
- Hamdi, S. E., A. Le Duff, L. Simon, G. Plantier, A. Sourice, and M. Feuilloley (2013). Acoustic emission pattern recognition approach based on Hilbert–Huang transform for structural health monitoring in polymer-composite materials. *Applied Acoustics* 74(5), 746–757.
- Marec, A., J.-H. Thomas, and R. El Guerjouma (2008). Damage characterization of polymer-based composite materials: Multivariable analysis and wavelet transform for clustering acoustic emission data. *Mechanical systems and signal processing* 22(6), 1441–1464.
- Nazmdar Shahri, M., J. Yousefi, M. Fotouhi, and M. Ahmadi Najfabadi (2016). Damage evaluation of composite materials using acoustic emission features and Hilbert transform. *Journal of Composite Materials* 50(14), 1897–1907.
- Oskouei, A. R., H. Heidary, M. Ahmadi, and M. Farajpur (2012). Unsupervised acoustic emission data clustering for the analysis of damage mechanisms in glass/polyester composites. *Materials & Design* 37, 416–422.
- Platt, J. (1999). Probabilistic outputs for support vector machines and comparisons to regularized likelihood methods. *Advances in large margin classifiers* 10(3), 61–74.
- Ren, Z., A. S. Verma, Y. Li, J. J. Teuwen, and Z. Jiang (2021). Offshore wind turbine operations and maintenance: A state-of-the-art review. *Renewable and Sustainable Energy Reviews* 144, 110886.
- Rothe, S., S. F. Wirtz, G. Kampmann, O. Nelles, and D. Söffker (2017). Ensuring the reliability of damage detection in composites by fusion of differently classified acoustic emission measurements. *Structural Health Monitoring* 2017, 1380–1387.
- Sayar, H., M. Azadi, A. Ghasemi-Ghalebahman, and S. M. Jafari (2018). Clustering effect on damage mechanisms in open-hole laminated carbon/epoxy composite under constant tensile loading rate, using acoustic emission. *Composite Structures* 204, 1–11.
- Sharmila Joseph, J., A. Vidyarthi, and V. P. Singh (2022). Multiclass image classification using oaa-svm. In *Machine Intelligence and Smart Systems*, pp. 235–244. Springer, Singapore.
- Tusar, M. I. H. and B. R. Sarker (2022). Maintenance cost minimization models for offshore wind farms: A systematic and critical review. *International Journal of Energy Research* 46(4), 3739–3765.
- Wang, C. and J. Zhang (2020). Experimental and analytical study on residual stiffness/strength of CFRP tendons under cyclic loading. *Materials* 13(24), 5653.
- Wirtz, S. F., N. Beganovic, and D. Söffker (2016). Experimental results of frequency-based classification of damages in composites. *8th European Workshop on Structural Health Monitoring* 21(8), 1–10.
- Wirtz, S. F., N. Beganovic, and D. Söffker (2019). Investigation of damage detectability in composites using frequency-based classification of acoustic emission measurements. *Structural Health Monitoring* 18(4), 1207–1218.
- Wu, T.-f., C.-J. Lin, and R. Weng (2004). Probability estimates for multi-class classification by pairwise coupling. *Journal of Machine Learning Research* 5, 975–1005.